

# Metallography: An Introduction

METALLOGRAPHY is the scientific discipline of examining and determining the constitution and the underlying structure of (or spatial relationships between) the constituents in metals, alloys and materials (sometimes called materialography). The examination of structure may be done over a wide range of length scales or magnification levels, ranging from a visual or low-magnification ( $\sim 20\times$ ) examination to magnifications over  $1,000,000\times$  with electron microscopes. Metallography may also include the examination of crystal structure by techniques such as x-ray diffraction. However, the most familiar tool of metallography is the light microscope, with magnifications ranging from  $\sim 50$  to  $1000\times$  and the ability to resolve microstructural features of  $\sim 0.2\ \mu\text{m}$  or larger.

The other major examination tool in metallography is the scanning electron microscope (SEM). Compared to the light microscope, the SEM expands the resolution range by more than two orders of magnitude to approximately  $4\ \text{nm}$  in routine instruments, with ultimate values below  $1\ \text{nm}$ . Useful magnification covers the range from the stereomicroscope, the entire range of the light microscope, to much of the range of the transmission electron microscope (TEM) for possible viewing from  $1,000\times$  to  $>100,000\times$ . The SEM also provides a greater depth of field than the light microscope, with depth of focus ranging from  $1\ \mu\text{m}$  at  $10,000\times$  to  $2\ \text{mm}$  at  $10\times$ , which is larger by more than two orders of magnitude compared to the light microscope (Table 1). This higher depth of field allows better discernment of topology features during a microscopic investigation, such as the examination of fracture surface during failure analysis. The depth of field of an SEM also may be a factor of choice over light microscopy, when very rough surfaces are being examined on a macroscopic level. For additional information on the comparative capabilities of light and electron microscopy, see the article “Light and Electron Microscopy” in this Volume.

However, even with the advent of electron microscopy, the light microscope is still the first and most important examination device in metallography. Sometimes the contrast in a microstructure is inadequate with a SEM under  $500\times$ , while it is highly visible with a basic light microscope and a properly prepared sample. Indeed, light microscopy is the historical and practical cornerstone of metallography, as described in the next section “The Origins of Metallogra-

phy,” which summarizes the basic discovery by Sorby demonstrating the importance of specimen preparation when examining metals with a light microscope. Contrast between microstructural constituents in light microscopy is very dependent on specimen preparation. Light microscopes also have various types of special illumination modes that can increase the information gained from the image (see the article “Light Microscopy” in this Volume). For example, polarized-light illumination can improve phase contrast, and the differential interference contrast (DIC) method can be used to identify topological height differences on a sample surface that are smaller than  $0.2\ \mu\text{m}$ .

The objective of these tools is to accurately reveal material structure at the surface of a sample and/or from a cross-section specimen. Examination may be at the macroscopic, mesoscopic, and/or microscopic levels. For example, cross sections cut from a component or sample may be macroscopically examined by light illumination in order to reveal various important macrostructural features (on the order of  $1\ \text{mm}$  to  $1\ \text{m}$ ) such as:

- Flow lines in wrought products
- Solidification structures in cast products
- Weld characteristics, including depth of penetration, fusion-zone size and number of passes, size of heat-affected zone, and type and density of weld imperfections
- General size and distribution of large inclusions and stringers
- Fabrication imperfections, such as laps, cold welds, folds, and seams, in wrought products
- Gas and shrinkage porosity in cast products
- Depth and uniformity of a hardened layer in a case-hardened product

Macroscopic examination of a component surface is also essential in evaluating the condition

of a material or the cause of failure. This may include:

- Characterization of the macrostructural features of a fracture surfaces to identify fracture initiation site and changes in crack-propagation process
- Estimations of surface roughness, grinding patterns, and honing angles
- Evaluation of coating integrity and uniformity
- Determination of extent and location of wear
- Estimation of plastic deformation associated with various mechanical processes
- Determination of the extent and form of corrosive attack; readily distinguishable types of attack include pitting, uniform, crevice, and erosion corrosion
- Evaluation of tendency for oxidation
- Association of failure with welds, solders, and other processing operations

This listing of macrostructural features in the characterization of metals, though incomplete, represents the wide variety of features that can be evaluated by light microscopy.

Mesoscale structure is on the order of  $1\ \text{mm}$  to  $100\ \mu\text{m}$ . It includes microstructural features at the grain level, without resolving the intricacies of the grain structure. For example, uniformity of case depth is an example of a mesoscale feature. Solidification structures at the mesoscale level include features such as cell sizes (eutectic cell), dendrites and arms, grain type (columnar or equiaxed), the type and concentration of chemical microsegregation, and the amount of microshrinkage, porosity, and inclusions. The term “mesoscale” is a relatively new term, introduced in part to more accurately distinguish between different scales.

Microstructure is the classic term used in metallography to describe features observed under a microscope in the scale range of  $1000\text{--}0.1\ \mu\text{m}$ .

**Table 1** Depth of field of typical light microscope objectives

Final magnification, diameters	Objective		Area of field(a), $\mu\text{m}$	Depth of field, $\mu\text{m}$
	Magnification, diameters	Numerical aperture		
100	5.6	0.20(b)	1000	20
250	8.0	0.40(b)	400	3
500	21.0	0.65(b)	200	1
750	41.0	0.85(b)	135	0.4
1000	58.0	0.95(b)	100	0.1
	50.0	1.0(c)	100	0.6
1500	75.0	1.4(c)	65	0.2

(a) For a final projected image  $10\ \text{cm}$  ( $4\ \text{in.}$ ) in diameter. (b) Dry objective. (c) Oil-immersion objective

## 4 / Introduction

The importance of microstructure to the properties of metals and alloys has long been recognized. Grain size, twins, and the size, shape, and distribution of second-phase particles are important in determining the behavior of most metals and alloys. These microstructural features are within the fundamental resolution limits of light of  $0.2\ \mu\text{m}$  (or greater). Then, if necessary, the examination may move to higher levels of magnifications with a scanning electron microscope, or a transmission electron microscope (TEM). For example, dislocations, numerous types of second-phase particles, spinodal and ordered structures, and many aspects of martensitic structures are too small for resolution by light microscopy. Therefore, metallographic observation of these very fine structural features is generally restricted to electron microscopy. The scale hierarchy of microstructural features is described in more detail in the article "Introduction to Structures in Metals."

### The Origins of Metallography

The critical factor in the light microscopy of metals is the surface preparation of the specimen. This is the basic insight discovered by the father of metallography, Henry Clifton Sorby (Fig. 1), who was the first person to examine correctly polished and chemically etched metal samples under the microscope in 1863 (Ref 1). This application of microscopy is more than two centuries later than the biological microscope, be-



**Fig. 1** Henry Clifton Sorby (1826–1908), geologist, petrographer, mineralogist, and founder of metallography. Source: Ref 6

cause the microscopy of metals requires careful preparation of the surface. Unlike biological samples, metals are opaque and thus require reflected light microscopy (where the impinging light for viewing is reflected off the specimen surface). In contrast, biological samples are transparent and thus can be examined by transmitted light (transmission microscopy). Sorby understood the need for proper surface preparation when examining metals by reflected-light microscopy. Prior to Sorby, samples were only "distorted fractures and brutally burnished or abraded surfaces" (Ref 2). He advised that "(the final) polish must not be one which gives bright reflection but one which may show all the irregularities of the material and is as far removed as possible from a burnished surface" (Ref 3).

The other piece of the metallographic puzzle is the art of etching. An extremely smooth surface appears nearly featureless when examined by reflected-light microscopy, because the light reflects uniformly from the surface and appears as a uniform contrast by human eye. Thus, techniques are needed to enhance contrast differences between the different phases of constituents. These methods include etching, thin-film formation, or special illumination modes with light microscopes (see the article "Contrast Enhancement and Etching" in this Volume). Of these, chemical recipes for etching the surface are the oldest of the various contrasting techniques. Etching even precedes Sorby by at least four centuries, as in the case of macroetching techniques to reveal the damask patterns of swords and various pieces of armor. Macroetching was also used to reveal the structure of polished meteorites, such as the famous Widman-



**Fig. 2** Macrograph of the Elbogen iron meteorite prepared in 1808 by Widmanstätten and Schreibers using heavy etching in nitric acid. After rinsing in water and drying, printer's ink was rolled on the etched surface, and the sample was pressed onto a piece of paper. Source: Ref 4

stätten structure discovered by count Alois von Widmanstätten, a geologist and museum curator in Vienna, and his coworker Carl von Schreibers in 1808. They etched various meteorites to show the outstanding crystalline patterns in the Elbogen iron meteorite that fell in 1751. An excellent example of their work is shown in Fig. 2 (from Ref 4).

Widmanstätten and Schreibers etched specimens that could be viewed with the naked eye, but Sorby was the first to etch specimens and observe the true microstructure with a microscope. Sorby first cut and polished his specimens to remove all "traces of roughness." After polishing, he used extremely dilute nitric acid to etch his specimens. He actually followed the progress of etching in order not to overetch the specimen. The critical factor in this procedure was Sorby's laborious preparation of specimens carried out by hand. The polished surfaces were etched in dilute nitric and were undoubtedly of a considerably higher standard than those of his contemporaries, such as Wedding and Martins in Germany (Ref 5), who were also attempting to reveal the microstructures of steels.

Sorby may not have realized the exact reasons for the success of his preparation methods, but more importantly, all of the structures reported by Sorby are still accepted as being correct structures. On 28 July 1863, Sorby recorded in his diary that he had "discovered" the structure of an iron. It was not until 1886 and 1887, however, that his results were recorded in a journal with a wide readership (Ref 1, 3). By careful observation he identified major microstructural constituents of ferrous materials (the constituents now known as graphite, cementite, pearlite,\* austenite, and the phosphide eutectic). He recognized that iron was composed of a number of crystal grains, and he also realized that iron underwent an allotropic change on heating. As noted by Samuels (Ref 6), these are awesome achievements considering that he started from scratch and that they were achieved after such a short period of investigation.

From this beginning, the importance of specimen preparation remains central today. Many deficiencies arise when the preparation methods are neglected. False structures (or artifacts) can arise from the preparation in many ways. In particular, Jose Ramon Vilella (Fig. 3) was the first to realize that artifacts were sometimes being observed due to the presence of a layer of "distorted or disturbed" metal formed during the early stages of surface preparation and not during polishing itself (Ref 7). He demonstrated that the true microstructure was seen only when the dis-

\*At the end of the 19th century, very fine pearlite unresolved in the light microscopes was referred to as "sorbite" in honor of Sorby. However, because it is not a new constituent, the term "sorbite" did not survive. The term "pearlite" survives to this day and is actually connected to Sorby, because he described the "pearly constituent," i.e., pearlite, as having a "mother of pearl" appearance.

turbed layer was removed, and he devised a method (alternate etching and polishing) of doing this (Fig. 4) (Ref 7).

Vilella's seminal work established the need for preparation procedures beyond just the production of reflecting surfaces. Successful metallography imposes the following requirements on the final preparation of the specimen surface (Ref 6):

- Surface layers that might obscure structural features must not be present.
- False structures that might be detected during a subsequent examination must not have been introduced.
- All desired fields of view must be coplanar within the depth-of-field limits of the system to be employed for examination.
- The surface must be adequately free from stains and other accidental blemishes.

With these basic objectives in mind, then the next question is determining the most effective mechanical, chemical, and/or physical methods of specimen preparation for the appropriate microscopic tool. These methods are described in more detail in the Section "Metallographic Techniques" of this Volume.

After a micrograph from a properly prepared specimen is obtained and recorded, the next challenge is to interpret, understand, and use the information contained on the recorded image. Interpretation of microstructural features requires an understanding of crystal structure, kinetics, and the metallurgical mechanisms of solidification, deformation, and phase transformations. These topics, as they relate to structure, are introduced in more detail in the series of articles



**Fig. 3** Jose Ramon Vilella (1897–1971), distinguished metallographer who understood the need to faithfully prepare representative surfaces in metallographic examinations. Source: Ref 6

in the next Section "Metallurgy and Microstructure." Interpretation of micrographs also requires an understanding of how specimen preparation and microscopic techniques affect the appearance of particular phases in a given material. Thus, the cataloging of micrographs (in print and/or electronic form) can be useful when comparing the effects of material variations and changes in specimen preparation.

### Macroanalysis (Adapted from Ref 8)

Macrostructural characterization of metals and alloys is the detailed evaluation of large-scale inhomogeneities in composition, morphology, and/or density. These inhomogeneities may develop during such procedures as casting, extrusion, forging, rolling, and welding or during service. Macroscale examination of surfaces is also essential in the failure analysis of fractured, corroded, and/or worn parts. Microscopic evaluation clearly is a significant step in any failure examination, but it should not replace characterization by macroscopy. These two types of metallography are complementary, but examination during failure analysis should always begin at low magnification and work upward. A frequent mistake in failure analysis is to neglect examination of the broken pieces at low magnifications. Too frequently, the component is sectioned immediately.

Examination techniques other than metallography may also be more effective during macroscale examination. For example, Fig. 5 shows spider cracks in the center of a copper specimen. This specimen was sectioned, ground, and polished, but not etched. Chemical etching and subsequent evaluation of the macrostructure may fail to reveal this type of structural imperfection (Fig. 5b). The cracks shown in Fig. 5(a) were

revealed by applying a dye penetrant to the polished specimen. The dye was drawn into the cracks by capillary action, and the surface was then wiped clean. The specimen was then placed under a light that caused the dye to fluoresce, and the cracks became readily observable. Dye-penetrant techniques are excellent for examination of cracklike macrostructural imperfections in metals. However, grains and other microstructural features are visible only after etching, which frequently obscures the presence of the cracks. Therefore, different metallographic techniques are necessary to reveal various macrostructural elements.

### Macroscopy of Sections

Preparation of a metallographic section for examination requires careful selection of the area to be characterized (see the article "Metallographic Sectioning and Specimen Extraction" in this Volume). This area must be chosen to represent the unique features of a specific zone of interest or the general features of a part or component selected for process characterization or quality assurance. The selected region of the specimen must then be removed from the component using techniques that do not damage or distort the features of interest. The section of interest is then prepared metallographically, and the prepared section is characterized using macroscopic examination.

Macroscopic examination generally does not require the extreme surface smoothness needed for microscopic examinations. Such surface preparation techniques as etching are frequently prolonged such that surface features are greatly enhanced; therefore, quantitative measurements should not be conducted on macroetched samples. Heavy etching accentuates any microstructural inhomogeneity (Fig. 6). The flow lines

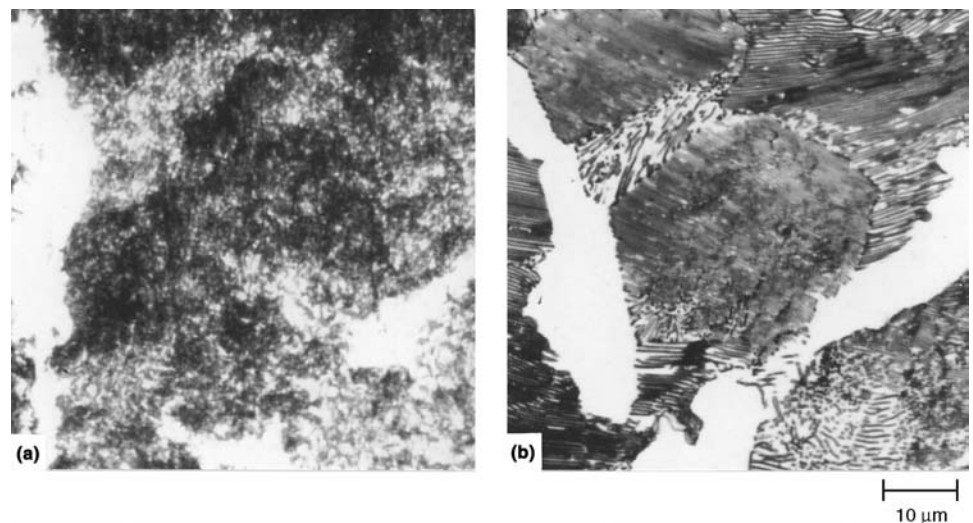


**Fig. 4** An example used by Vilella to illustrate the effect of disturbed metal on the appearance of pearlite. (a) Polished surface covered by a layer of disturbed metal; structures such as this were called sorbite or troostite-sorbite by some early investigators. (b) Same field after removing the layer of disturbed metal by alternate polishing and etching; true structure of lamellar pearlite. Etched in picral reagent. 1000 $\times$ . Source: Ref 7

## 6 / Introduction

show the direction of metal flow during processing and frequently represent paths for easy fracture. Figure 7 shows the use of similar macroscopic techniques to illustrate the depth of case hardening in a tool steel. Figure 8 is a weld macrograph that shows the different etching characteristics of the fusion zone and heat-affected zone (HAZ) of a weld. The 2% nital etchant used to reveal the weld macrostructure is much less aggressive than the 50% hydrochloric acid etchants used on the specimens shown in Fig. 6 and 7 and reveals finer structural detail but requires a polished specimen.

In castings, macroscopy is used to establish the outer chill zone depth, shape, and size of the columnar or dendritic grains perpendicular to the mold wall, and size of the central equiaxed zone (Fig. 9). For example, Fig. 10 shows the macrostructure of a small, relatively pure aluminum ingot exhibiting typical cast grain structure. To obtain the macrograph, the aluminum ingot was sectioned, then ground and polished to produce a flat reflective surface. The polished section was then etched by immersion in a solution that attacked the various grain orientations at different rates. The structural elements visible in this macrograph are grains. The small grains near the bottom of the ingot appear relatively equiaxed. This region of small equiaxed grains is the chill zone. Macroscopy of cast structures is also used to reveal imperfections such as shrinkage, gas, porosity, and center cracks.

### Macroscopy of Fracture Surfaces (Adapted from Ref 9)

Both the macroscale and macroscale appearances of fracture-surface features can tell a story of how and sometimes why fracture occurred.

Features often associated with the fracture surface at the macroscale and macroscale are shown in Tables 2 and 3. Examination of the information in these tables shows that the fracture features provide information about (Ref 9):

- The crack-initiation site and crack-propagation direction
- The mechanism of cracking and the path of fracture
- The load conditions (monotonic or cyclic)
- The environment
- Geometric constraints that influenced crack initiation and/or crack propagation
- Fabrication imperfections that influenced crack initiation and/or crack propagation

It should also be clear that not all features created by a given cause for failure are necessarily present on a given fracture surface. For example, beach marks (at low magnification) and striations (at higher magnification) are well-known features of fatigue cracks, but are not always present or visible. In addition, not all fracture mechanisms have unique appearances. For example, intergranular fracture can be caused by a number of mechanisms.

It is also important to understand that the fracture surface only provides evidence of the crack-propagation process; it does not reveal evidence of events prior to nucleation and growth. Examination beyond the fracture surface also provides information. For example, visual inspection of a fractured component may indicate events prior to fracture initiation, such as a shape change indicating prior deformation. Metallographic examination of material removed far from the fracture surface also can provide information regarding the penultimate microstructure, including the presence of cold work (slip, bent annealing twins, deformation bands, and/or grain shape change), evidence of rapid loading

and/or low-temperature service (deformation twins), and so forth. This also is very necessary to the failure investigation.

Macroscopic features typically help identify the fracture-initiation site and crack-propagation direction. The orientation of the fracture surface, the location of crack-initiation site(s), and the

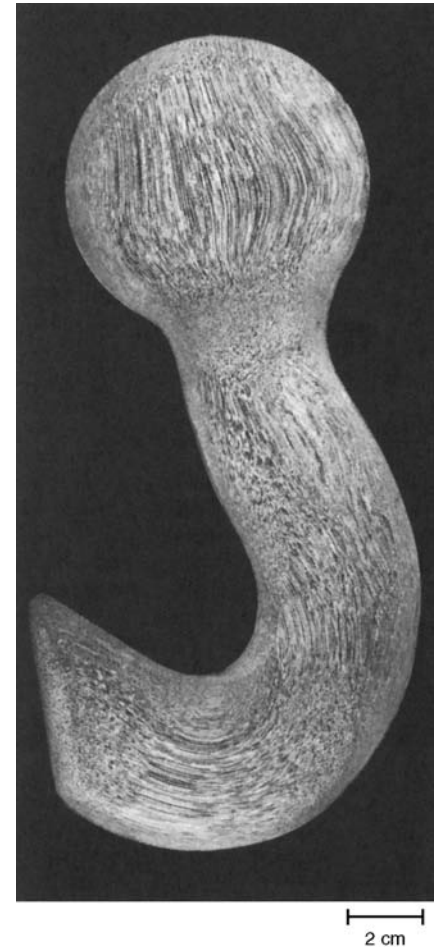


**Fig. 6** Flow lines in a forged 4140 steel hook. Specimen was etched using 50% HCl. 0.5 $\times$ . Source: Ref 8

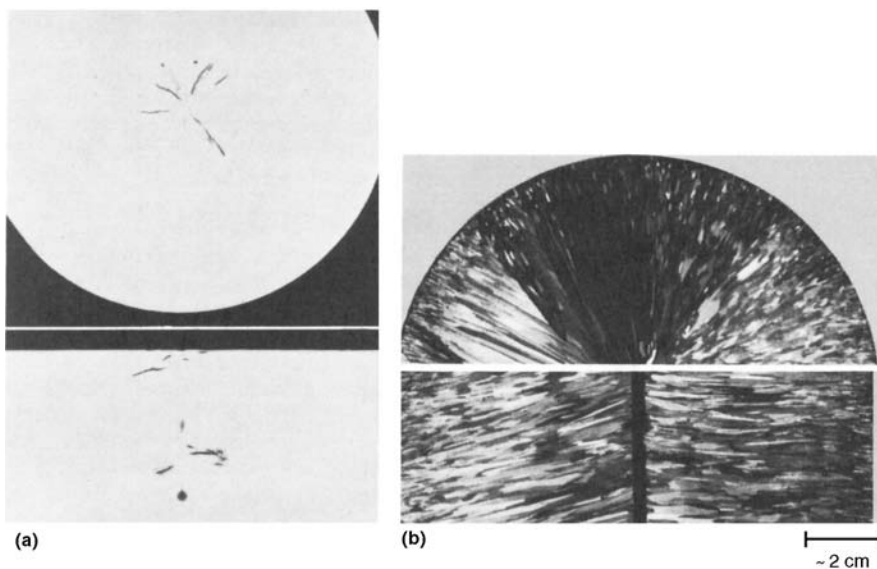


**Fig. 5** Macrostructure of a continuous-cast copper ingot. (a) Spider cracks revealed using dye-penetrant inspection. Transverse section at top; longitudinal section at bottom. (b) Same ingot, etched using Waterbury's reagent. Cracks are not revealed. Both approximately 0.5 $\times$ . Source: Ref 8

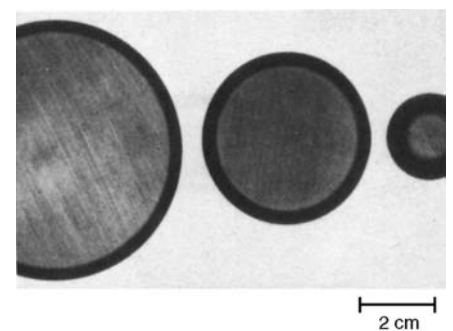


**Fig. 7** Case-hardened layer in W1 tool steel. Specimens were austenitized at 800  $^{\circ}$ C (1475  $^{\circ}$ F), brine quenched, and tempered 2 h at 150  $^{\circ}$ C (300  $^{\circ}$ F). Black rings are hardened zones. Etched using 50% hot HCl. Approximately 0.5 $\times$ . Source: Ref 8

crack-propagation direction should correlate with the internal state of stress created by the external loads and component geometry. When

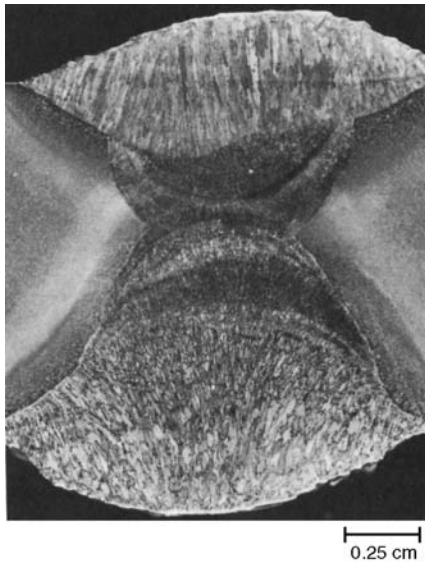


**Fig. 8** Section through an arc butt weld joining two 13 mm (0.5 in.) thick ASTM A517, grade J, steel plates. Etched using 2% nital. 4×. Source: Ref 8

the failed component is in multiple pieces, and chevrons are visible on the fracture surface, analysis of crack branching (crack bifurcation) (Fig. 11) (Ref 10) can be used to locate the crack-initiation site. Fracture initiates in the region where local stress (as determined by the external loading conditions, part geometry, and/or macroscopic and microscopic regions of stress concentration) exceeds the local strength of the material. Thus, variations in material strength and microscale discontinuities (such as an inclusion or forging seam) must be considered in conjunction with variations in localized stress that is determined by applied loads and macroscopic stress concentrations (such as a geometric notch or other change in cross section).

The fracture surface orientation relative to the component geometry may also exclude some loading conditions (axial, bending, torsion, monotonic versus cyclic) as causative factors. For example, crack initiation is not expected along the centerline of a component loaded in bending or torsion, even if a significant material imperfection is present at that location because no normal stress acts at the centerline. (There is a shear stress at this location in bending, but in a homogeneous material, it is too small to initiate

fracture. That might not be the case for a laminated structure loaded in bending.)

Likewise, the profile of a fracture surface relative to loading direction can indicate the mode of fracture by elastic (plane-strain) conditions or elastic-plastic (plane-stress) conditions. Plane-strain (or mode I) fracture is characterized by a flat surface perpendicular to the applied load. Plane-stress (mode II) fracture occurs when shear strain becomes the operative mode of deformation and fracture (as maximum stresses occur along the shear plane from the basic principles of continuum mechanics). In plane-stress cracking, the fracture profile is characterized by shear lips, which are at about a 45° oblique angle to the maximum stress direction (although this angle may vary depending on material condition and loading condition). In general, these variations in fracture profiles are related to fracture toughness, which depends on section thickness (*B*) and the size (*a*) of a preexisting discontinuity such as a notch. This is shown in Fig. 12. Crack-tip radius also influences fracture behavior.

Surface roughness and optical reflectivity also provide qualitative clues to events associated with crack propagation. For example, a dull/matte surface indicates microscale ductile frac-

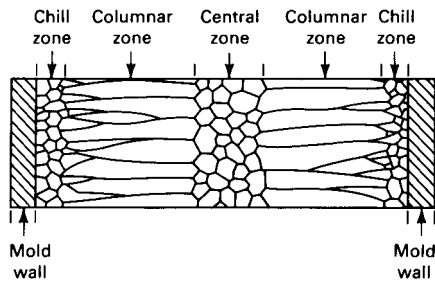


**Fig. 9** Sketch of grains in a typical cast ingot

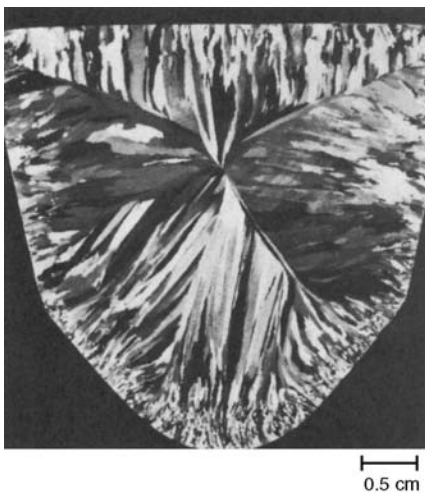


**Fig. 10** Macrostructure of as-cast aluminum ingot. Transverse section shows outer chill zone and columnar grains that have grown perpendicularly to the mold faces. Etched using Tucker's reagent. 1.5×. Source: Ref 8

**Table 2** Macroscale fractographic features

Mark/Indication	Implication
Visible distortion	Plastic deformation exceeded yield strength and may indicate instability (necking, buckling) or post-failure damage
Visible nicks and gouges	Possible crack initiation site
Fracture surface orientation relative to component geometry and loading conditions	<ul style="list-style-type: none"> <li>• Helps separate loading modes I, II, III</li> <li>• Identifies macroscale ductile and brittle fracture.</li> </ul>
Both flat fracture and shear lips present on fracture surface	<ul style="list-style-type: none"> <li>• Crack propagation direction parallel to shear lips</li> <li>• Mixed-mode fracture (incomplete constraint)</li> </ul>
Tightly closed crack on surface	<ul style="list-style-type: none"> <li>• Possible cyclic loading</li> <li>• Possible processing imperfection, e.g., from shot peening, quench cracks</li> </ul>
Radial marks and chevrons (V-shape)	<ul style="list-style-type: none"> <li>• Point toward crack initiation site</li> <li>• Show crack propagation direction</li> </ul>
Crack arrest lines (monotonic loading) (U-shape)	<ul style="list-style-type: none"> <li>• Lines point in direction of crack propagation</li> <li>• Indicate incomplete constraint</li> </ul>
Crack arrest lines (cyclic loading) (beach marks, conchoidal marks)	<ul style="list-style-type: none"> <li>• Indicates cyclic loading</li> <li>• Propagation from center of radius of curvature</li> <li>• Curvature may reverse on cylindrical sections as crack propagates</li> <li>• More likely in cyclic loading</li> </ul>
Ratchet marks	<ul style="list-style-type: none"> <li>• Indicates initiation site(s)</li> </ul>
Adjacent surface and or fracture surface discoloration	<ul style="list-style-type: none"> <li>• May indicate corrosive environment</li> <li>• May indicate elevated temperature</li> </ul>
Oxidized fingernail on fracture surface	Possible crack initiation site
Fracture surface reflectivity	<ul style="list-style-type: none"> <li>• <i>Matte</i>: ductile fracture or cyclic loading</li> <li>• <i>Shiny</i>: cleavage likely</li> <li>• Faceted ("bumpy") and shiny; intergranular fracture in large grain size</li> </ul>
Fracture surface roughness	<ul style="list-style-type: none"> <li>• Increase in surface roughness in direction of crack growth (may be affected in bending by compressive stressed region when crack moves into this region)</li> <li>• Smooth region plus rough region in direction of growth—cyclic loading</li> </ul>
Rubbing (general)	<ul style="list-style-type: none"> <li>• Rough matte fractures are ductile</li> <li>• May indicate transition from fatigue crack growth to overload</li> <li>• May indicate vibration</li> </ul>
Rubbing (localized)	<ul style="list-style-type: none"> <li>• May show final direction of separation</li> <li>• Swirl pattern indicates torsion</li> <li>• May indicate crack closure in cyclic loading</li> <li>• May obliterate beach marks</li> </ul>
Deformed draw marks, rolling scratches	If twisted, indicates torsion loading
Machining marks (normal to axis of component)	Not distorted in torsion loading
Variable roughness of fracture edge	In brittle bending, rough side is tension side

Source: Ref 9

ture, while a shiny, highly reflective surface indicates brittle cracking by cleavage or intergranular fracture. In addition, when intergranular fracture occurs in coarse-grained materials, individual equiaxed grains have a distinctive rock-candy appearance that may be visible with a hand lens. In terms of documenting surface conditions, one major problem with optical (light) macroscopic or microscopic examination of fracture surfaces is its inability to obtain favorable focus over the entire surface if the magnification exceeds 5 to 10X. Therefore, SEM also has become a standard metallographic tool in failure analysis.

Surface roughness provides clues as to whether the material is high strength (smoother) or low strength (rougher) and whether fracture occurred as a result of cyclic loading. The surfaces from fatigue crack growth are typically smoother than monotonic overload fracture areas. The monotonic overload fracture of a high-strength quenched-and-tempered steel is significantly smoother overall than is the overload

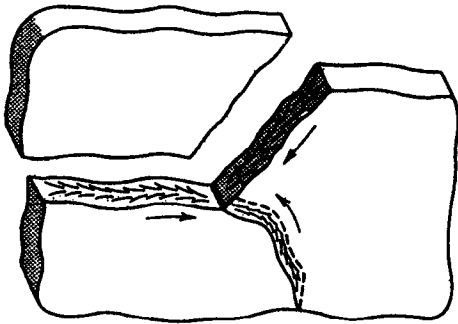


**Fig. 11** Component that has fractured in multiple pieces. If chevrons are visible on the fracture surface, the sequence of crack formation can be used to obtain the crack formation of sequence and the location of the initiation site. Source: Ref 10

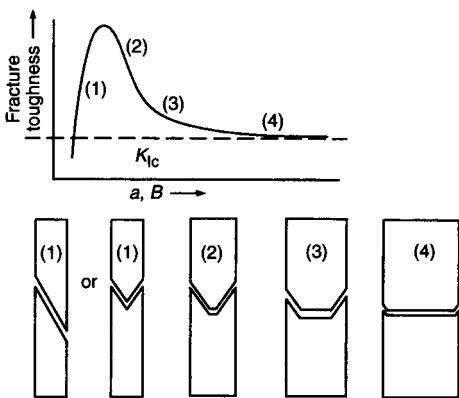


**Fig. 12** Variation in fracture toughness and macroscale features of fracture surfaces for an inherently ductile material. As section thickness ( $B$ ) or preexisting crack length ( $a$ ) increases, plane-strain conditions develop first along the centerline and result in a flat fracture surface. With further increases in section thickness or crack size, the flat region spreads to the outside of the specimen, decreasing the widths of the shear lips. When the minimum value of plane-strain toughness ( $K_{Ic}$ ) is reached, the shear lips have very small width. Source: Ref 9

fracture of a pearlitic steel or annealed copper. Also, fracture surface roughness increases as a crack propagates so the roughest area on the fracture surface is usually the last to fail. Fracture surface roughness and the likelihood of crack bifurcation also increase with magnitude of the applied load and depend on the toughness of the material. Brittle failures often contain multiple cracks and separated pieces, while ductile overload failures often progress as single cracks, without many separated pieces or substantial crack branching at the fracture location.

Under the right conditions, fracture surfaces may also have radial marks and chevrons, which are macroscopic surface features that indicate the region of crack initiation and propagation direction. They are common and dominant macroscopic features of the fracture of wrought metallic materials, but are often absent or poorly

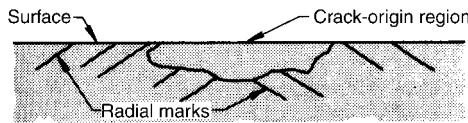


**Fig. 13** Radial marks typical of crack propagation that is fastest at the surface (if propagation is uninfluenced by the configuration of part or specimen)

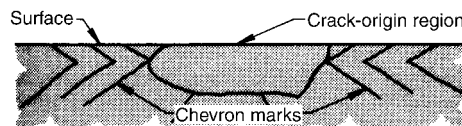


**Fig. 14** Chevron patterns typical when crack propagation is fastest below the surface. It is also observed in fracture of parts having a thickness much smaller than the length or width (see middle illustration in Fig. 15).

defined in castings. The “V” of a chevron points back to the initiation site, and a sequence of “V”s across the fracture surface indicates the crack-propagation direction. The appearance of chevrons or radial marks near the crack origin depends in part on whether the crack-growth velocity at the surface is greater or less than that below the surface. If crack-growth velocity is at a maximum at the surface, radial marks have a fan-shaped appearance (Fig. 13). If crack-growth rate is greatest below the surface, the result is chevron patterns (Fig. 14).

In rectangular sections, specimen dimensions can affect the appearance of radial markings and chevron patterns. For example, the macroscale fracture appearances of unnotched sections are shown in Fig. 15 for sections with various width-

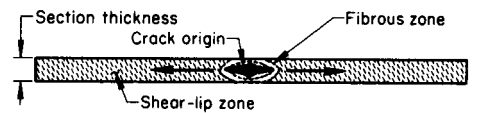
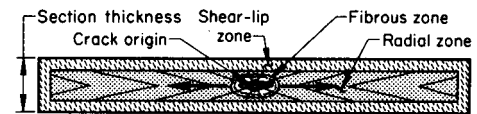
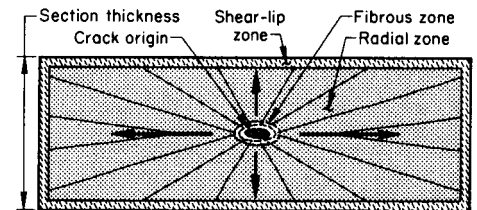


**Fig. 15** Typical fracture appearances for unnotched prismatic tension-test sections. Source: Ref 9

**Table 3** Microscale fractography features

Mark/Indication	Implication
Dimpled fracture surface	Ductile overload fracture at this location
Faceted fracture surface	<ul style="list-style-type: none"> <li>• Brittle cleavage fracture</li> <li>• Possible SCC fracture</li> <li>• May be low <math>\Delta K</math> fatigue</li> </ul>
Intergranular with smooth grain boundaries	<ul style="list-style-type: none"> <li>• Likely either improper thermal processing or environmental assisted fracture (high temperature, corrosive environment)</li> <li>• Less common is low <math>\Delta K</math> fatigue</li> </ul>
Intergranular with dimpled grain boundaries	<ul style="list-style-type: none"> <li>• “Decohesive” rupture—fracture at high fraction of melting point</li> <li>• Possible improper processing creating denuded zone adjacent to grain boundary</li> </ul>
River pattern or fan pattern	Cleavage fracture; crack runs “down” river; fan rays point to initiation site within a grain.
Tongues	Twinning deformation during rapid crack propagation
Flutes on transgranular fracture surface	<ul style="list-style-type: none"> <li>• Indicates corrosive environment and ductile fracture</li> <li>• Crack propagates parallel to flutes.</li> <li>• Cyclic loading fatigue striations; Constant spacing, constant stress amplitude; variable spacing, variable stress amplitude or block loading</li> </ul>
Striated or ridged fracture	<ul style="list-style-type: none"> <li>• Striated surface caused by second phases in microstructure.</li> <li>• SCC</li> <li>• Transgranular fracture</li> </ul>
Grooves or flutes	Dried liquid on surface. May indicate incomplete cleaning of surface. If in the as-received condition, may indicate fluids from service and may indicate SCC conditions. Material should be analyzed.
Artifacts (mud cracks)	<ul style="list-style-type: none"> <li>• Common in cyclic loading</li> <li>• Due to entrapped particulate matter</li> </ul>
Artifacts (tire tracks)	

Source: Ref 9

to-thickness ( $w/t$ ) ratios. The  $w/t$  ratio influences the ability of the sample to maintain a unidirectional state of stress during tension. In a thick section (top), strain in the width direction is constrained and thus tends to a condition of plane-strain (mode I) fracture. In this case, a large portion of the fracture surface comprises radial markings or chevron patterns indicative of rapid, unstable cracking. At higher  $w/t$  ratios, the radial zone is suppressed in favor of a larger shear-lip zone. In very thin sections (bottom), plane-stress conditions apply, and the fracture surface is composed almost entirely of a shear lip outside the fibrous zone of crack initiation. Figure 16 shows radial marks and chevrons when fracture initiates from surface notches.

If conditions are right, the radial patterns associated with rapid or unstable crack propagation can also occur in a cylindrical section. This radial pattern, sometimes called a radial shear, star,

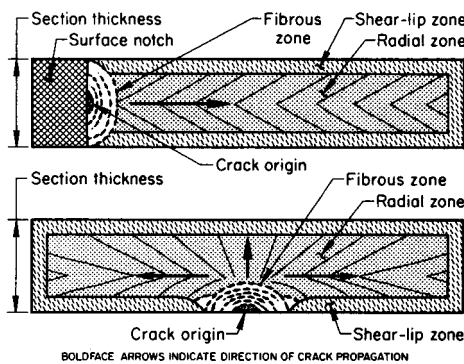


**Fig. 16** Typical fracture appearances for edge- and side-notched rectangular tension-test sections. Note the shear lips when the fracture approaches the edge of the specimen. Source: Ref 9

or rosette, is perpendicular to the crack front and, as such, may be considered to be the round-sample equivalent of the radial markings or chevron patterns that appear on sheet or plate samples, as previously described. The radial marks, or radial shear marks, are visually distinct from the fibrous region, as shown in Fig. 17 for an unnotched SAE 4150 steel specimens with different strengths. Figure 17(a) shows a clear boundary between the fibrous central region and the large ridge pattern of the radial marks. Figure 17(b) shows shallower radial marks and a slightly larger fibrous zone from a heat treatment that results in more ductility. Figure 17(c) shows very weak or shallow radial marks that develop further from the center.

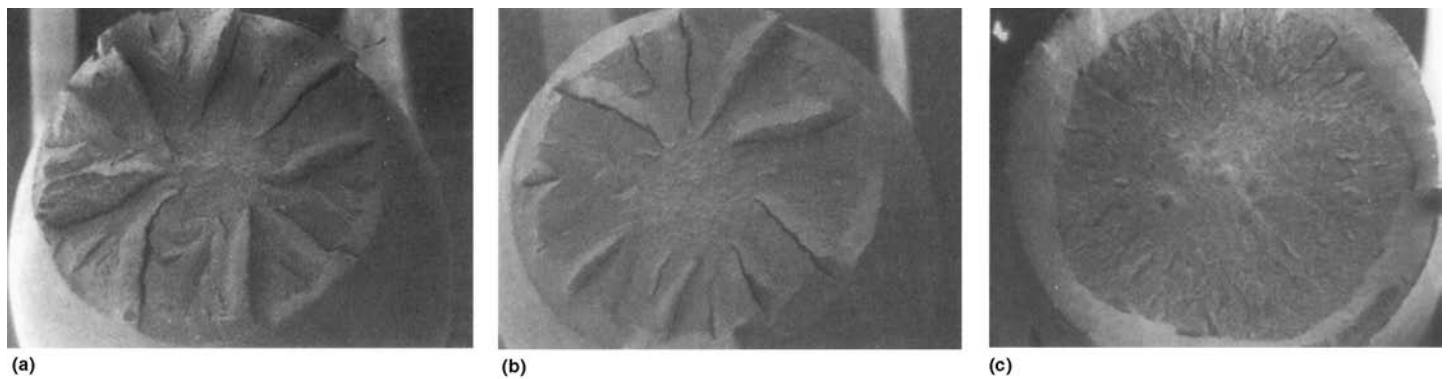
Radial marks on the fracture surface of an unnotched cylindrical tension-test specimen (Fig. 18) point to the center, which has a fibrous appearance that is associated with ductile crack initiation and growth by microvoid coalescence. However, if the specimen is notched (Fig. 18b), then crack initiation may begin at several locations along the circumference near the root of the notch, where stress concentration occurs. The region of crack initiation may still have a fibrous appearance indicative of microvoid coalescence (MVC) near the root of the notch, but the region of final, fast fracture is in the center and roughly perpendicular to the applied load. Thus, even though the radial markings may appear to point to the center, the surface conditions indicate that the central region is the area of final fracture, not crack initiation. In effect, the notch size is sufficient to cause plane-strain fracture, as evidenced by the lack of shear lips.

**Macroscopic Appearance of Ductile Fractures.** As noted in Table 2, ductile fractures are typically characterized by evidence of plastic deformation, such as necking of a tension-test

specimen. Ductile fractures often progress as single cracks, without many separated pieces or substantial crack branching at the fracture location. The region of a crack-initiation typically has a dull fibrous appearance that is indicative of cracking by MVC. The crack profiles adjacent to the fracture are consistent with tearing. The fracture surface may have radial markings, chevrons, and/or shear lips depending on the specimen geometry and material condition, as previously noted.

An example of mixed-mode (mode I and II) fracture is the classic cup-and-cone appearance from ductile fractures of unnotched cylindrical tension-test specimen (Fig. 18a). In this case, the fracture originates near the specimen center, where hydrostatic stresses develop during the onset of necking and where microvoids develop and grow. Multiple cracks join and spread outward along the plane normal to loading axis, as representative of mode I (plane-strain) crack propagation. When cracks reach a region near the outer surface, the mode of fracture changes to mode II (plane-stress) condition, where shear strain becomes the operative mode of deformation. Thus, even though the overall applied stress is still a tensile load, deformation makes a transition to the shear plane in the outer regions of the specimen and thus results in the 45° shear lips that are indicative of a mode II fracture. Alternatively, the fracture mode may be entirely plane strain when a sufficiently large crack or notch is introduced (Fig. 18b).

**Macroscopic Appearances of Brittle Fractures.** Brittle overload failures, in contrast to ductile overload failures, are characterized by little or no macroscopic plastic deformation. Brittle fracture initiates and propagates more readily than ductile fracture or so-called “subcritical” crack-propagation processes such as fatigue or



Specimen	Hardness, HV	Yield strength		Ultimate tensile strength		Reduction of area, %	Charpy V-notch impact energy		Fibrous zone as percentage of total area
		MPa	ksi	MPa	ksi		J	ft · lbf	
(a)	285	0.73	0.106	0.83	0.120	66	163	120	~25
(b)	258	0.65	0.094	0.79	0.115	67	174	128	~31
(c)	301	0.81	0.117	0.97	0.141	49	27	20	~44

**Fig. 17** Radial marks on tensile test specimen of Society of Automotive Engineers (SAE) 4150 steel isothermally transformed to bainite, quenched to room temperature, and then tempered. (a) Lower bainite, isothermally transformed at 300 °C (570 °F) for 1 h, tempered at 600 °C (1110 °F) for 48 h. (b) Lower bainite, isothermally transformed at 375 °C (705 °F) for 1 h, tempered at 600 °C (1110 °F) for 48 h. (c) Upper bainite, isothermally transformed at 450 °C (840 °F) for 24 h, as-quenched. Source: David Johnson, Master’s thesis, University of Tennessee

stress-corrosion cracking. Because brittle fractures are characterized by relatively rapid crack growth, the cracking process is sometimes referred to as being “unstable” or “critical” because the crack propagation leads quickly to final fracture.

The macroscopic behavior is essentially elastic up to the point of failure. The energy of the failure is principally absorbed by the creation of

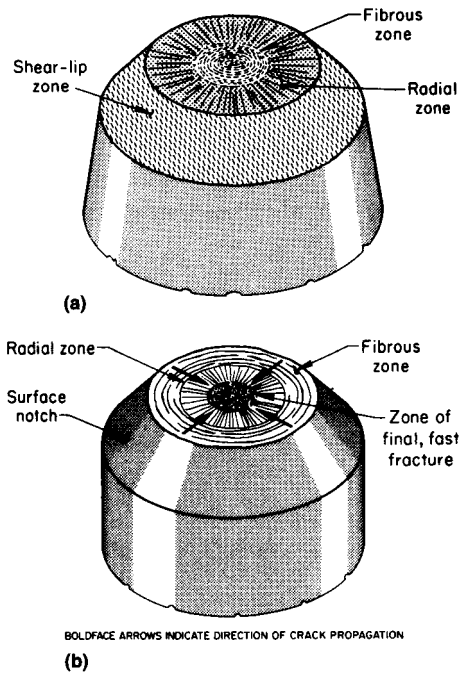


**Fig. 18** Fracture surface regions in cylindrical tension-test specimens. (a) Surface from cone portion of fractured unnotched tensile specimen. (b) Surface of fractured notched specimen. Unlike the fracture surface for an unnotched specimen, the fracture surface for the notched specimen (b) does not have shear lips, because the fracture initiates near the root of the notch (and completely around the specimens in this idealized case without additional stress raisers). Source: Ref 9

new surfaces, that is, cracks. For this reason, brittle failures often contain multiple cracks and separated pieces, which are less common in ductile overload failures. Brittle fracture mechanisms may exhibit chevron or herringbone patterns that indicate the fracture origin and direction of rapid fracture. Chevrons occur mainly in structural steels and rail (web) steel or relatively ductile low-strength alloys. Chevrons are dependent on strength, ductility, and section thickness, and are not normally seen in high strength alloys.

Herringbone patterns are unique microscopic features of brittle fractures (Ref 9). Ductile cracking, which occurs by microvoid coalescence, does not result in a herringbone pattern. On a microscopic scale, the features and mechanisms of fracture may have components of ductile or brittle crack propagation, but the macroscopic process of fracture is characterized by little or no work being expended from deformation.

**Macroscopic Appearances of Fatigue Fractures (Adapted from Ref 11).** Examination of a fatigue fracture usually begins with unaided visual observation, often followed by viewing with a hand lens or stereomicroscope. Macroscopic examination of fracture surfaces can be performed on-site (when the broken part is accessible), requires little or no preparation of the specimen, and uses minimal and relatively simple equipment. It does not destroy the specimen or alter fracture surfaces. Macroscopic examination is particularly useful in correlating fracture surface characteristics with part size and shape and with loading conditions.

Fatigue origins are frequently located most readily by viewing the fracture surface at low magnifications (up to 30 to 50 $\times$ ). For example, Fig. 19 shows a fracture of a steel housing tube. The initiation region is observable in the macrograph, as shown by the arrow. The position of the crack front at various times during the failure process is also visible as the so-called beach

marks that are initially fairly concentric to the origin.

Macroscopically, fatigue fracture ordinarily has a brittle appearance and lacks the gross plastic deformation (e.g., necking) characteristic of ductile tensile overload fracture. In contrast with ductile overload fracture, which generally has more-or-less shear lip (slant 45 $^\circ$  fracture) along free surfaces, propagating fatigue fractures typically intersect free surfaces at right angles (Fig. 20). This provides a tool for helping to identify fatigue locations. In common with other progressive fracture modes, such as stress-corrosion cracking, field fatigue fractures are frequently decorated by more-or-less curved marks that delineate the position of the crack front at a particular point in time. These marks are commonly called beach marks and are also known as clamshell marks or arrest marks.

Beach marks are produced by a change in crack-growth conditions, such as a change in environment or stress level or a pause in stress cycling (interruption in service). Thus, beach marks are not always present on the surface of a fatigue fracture. For example, beach marks are not found in laboratory tests conducted under uniform loading and environmental conditions (e.g., Fig. 20). Moreover, the presence of beach marks also is not conclusive evidence of fatigue fracture. Beach marks may also appear when fracture is from stress-corrosion cracking Fig. 21 (Ref 12).

## Microscopic Examination

The importance of microstructure to the properties of metals and alloys has long been recognized. Grain size, twins, and the size, shape, and distribution of second-phase particles are important in determining the behavior of most structural metals. Therefore, characterization of microstructures by light microscopy is essential. Process-control parameters are established to

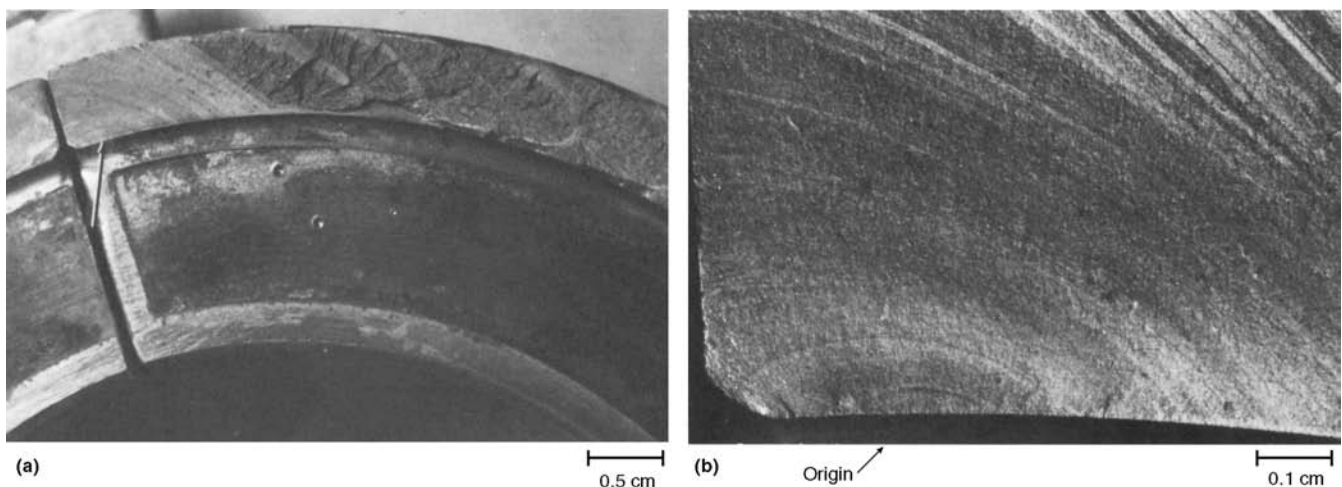


**Fig. 19** Fractographs of a typical fatigue crack in a clamp. (a) The fatigue crack origin is marked by the arrow. The crack propagated to the right by continuous fatigue cracking (light) region, then continued alternately by rapid tearing and slow fatigue cracking. 2 $\times$ . (b) Higher-magnification view of the region near the arrow in (a). 10 $\times$ . Source: Ref 8

provide specific grain sizes. The number, size, and distribution of second-phase particles, such as inclusions, are frequently specified, and quantitative metallographic procedures have been developed to describe microstructure.

This section on microanalysis focuses mainly on the method of light microscopy with some discussion of SEM in fractography. As previously noted, the upper limit of useful magnification in a light microscope is approximately  $1500\times$ , and the fundamental limitations of light optic systems limit resolution to features that are  $\sim 0.2\ \mu\text{m}$  or larger. Light microscopy, then, is used primarily to examine grain structures and the morphology of large second-phase particles. However, many other microstructural features that are too small to be observed using light microscopy also can influence the properties of metals and alloys. Dislocations, numerous types of second-phase particles, spinodal and ordered structures, and many aspects of martensitic structures can be categorized as too small for light microscopy. These features require examination by electron microscopy, which are discussed elsewhere (see the articles “Scanning Electron Microscopy” and “Transmission Electron Microscopy” in this Volume).

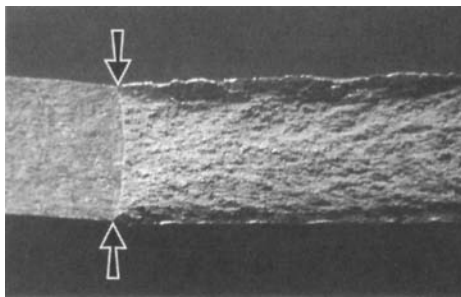


**Fig. 20** Aluminum alloy fracture mechanics test specimen, 6.3 mm (0.25 in.) thick. Fatigue crack at left of arrows is flat and perpendicular to side surfaces (note absence of beach marks in this laboratory fatigue fracture). Overload fracture to right of arrows has 45° shear lips extending upward at the top side of the sample and downward at the bottom side. Source: Ref 11

Microscopy is also essential in the analysis of failures due to fracture, wear, and/or corrosion. These topics and the use of light and electron microscopy in failure analysis are discussed in more detail in *Failure Analysis and Prevention*, Volume 11 of *ASM Handbook*. However, the section “Microfractography” in this article briefly compares the application of light and electron microscopy in fractographic analysis. Another important technique in microanalysis is replica metallography, where specimens are replicas taken in situ from components in the field. There

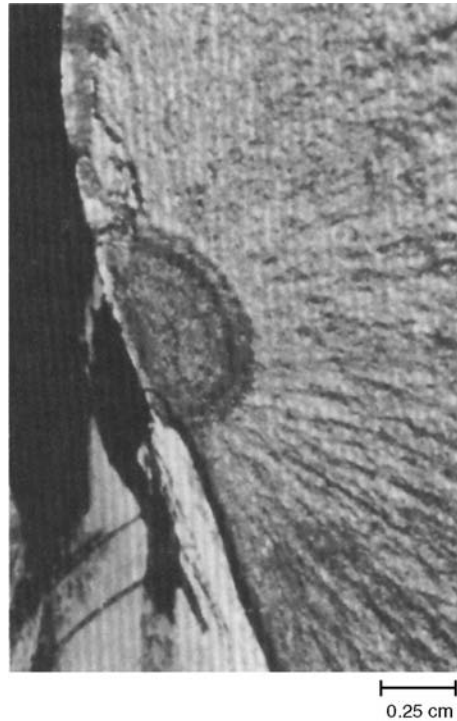


**Fig. 21** Beach marks on a 4340 steel part caused by stress-corrosion cracking. Tensile strength of the steel was approximately 1780 to 1900 MPa (260 to 280 ksi). The beach marks are a result of differences in the rate of penetration of corrosion on the surface. They are in no way related to fatigue marks.  $4\times$

are two types of replicas: surface replicas and extraction replicas. Surface replicas provide an image of the surface topography of a specimen, while extraction replicas lift particles from the specimen. The application of replica metallography is discussed in more detail in the article “Field Metallography Techniques” in this Volume.

### Microstructure

Optical (light) characterization of the microstructures of metals and alloys involves the identification and measurement of phases, precipitates, and constituents, and the determination of the size and shape of the grains, the extent of twinning, and some of the characteristics of grain boundaries and other observable defects. Solidification, solid-state transformation, deformation, and annealing microstructures are the four basic types in metals and alloys. Each of these has distinct characteristics, as described below. Anisotropy of grain orientation is also important when characterizing the microstructure of a material.

**Anisotropy.** Microstructural features exist in three dimensions, while metallographic observation typically represents only two dimensions. Therefore, effective microscopy frequently requires microstructural observations in two or more directions. For example, Fig. 22 and 23 illustrate the value of viewing the microstructure in several directions. Figure 22 shows an annealed microstructure exhibiting similar grain shapes in all three views. Grain size is characterized by placing a line of known length (or preferably a circle of known circumference) on the magnified image of the microstructure and counting the number of intersections between the line and grain boundaries in the microstructure. The number of grain boundary intersections,  $P$ , can be converted to a measure of grain size,  $l$ , using:

$$l = \frac{L}{PM} \quad (\text{Eq 1})$$

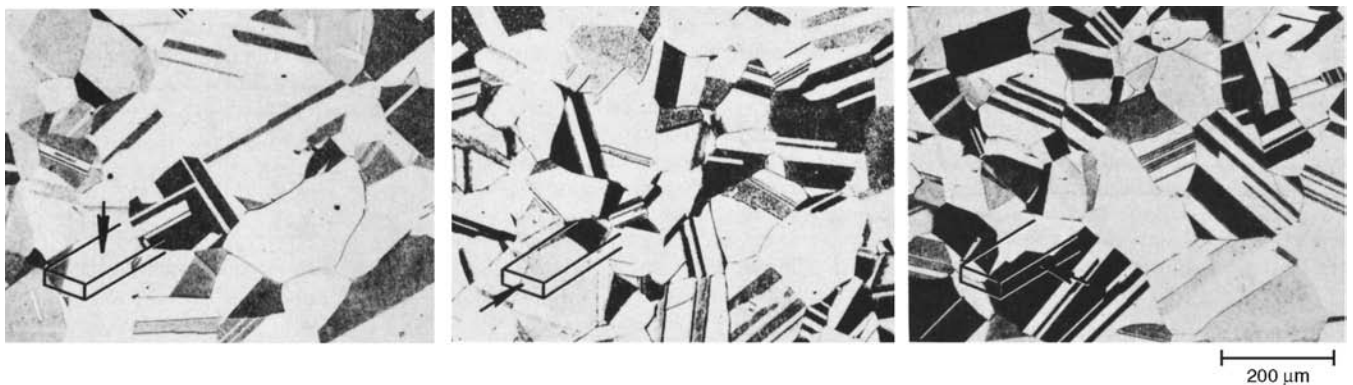


**Fig. 22** Copper alloy 26000 (cartridge brass, 70%) sheet, hot rolled to a thickness of 10 mm (0.4 in.), annealed, cold rolled to a thickness of 6 mm (0.230 in.), and annealed to a grain size of 0.120 mm (0.005 in.). At this reduction, grains are basically equiaxed. Compare with Fig. 23. Diagram in lower left of each micrograph indicates orientation of the view relative to the rolling plane of the sheet. Etched using  $\text{NH}_4\text{OH}$  plus  $\text{H}_2\text{O}_2$ .  $75\times$ . Source: Ref 8

where  $M$  is the magnification of the image observed,  $L$  is the length of line on the image, and grain size ( $l$ ) is the mean linear intercept length (per ASTM E112). The microstructure of the annealed alloy (Fig. 22) is isotropic, while the grains are elongated in the rolling direction and flattened in the transverse directions when alloy is in the cold-rolled condition. This anisotropic grain structure also renders anisotropic mechanical properties. Physical properties may also be anisotropic, especially in single-phase alloys due to texture. Thus, anisotropic materials may require selection, preparation, and viewing of specimens from different orientations. This is discussed further in the article “Metallographic Sectioning and Specimen Extraction” in this Volume. Modern techniques also include methods of three-dimensional representation (see the article “Three-Dimensional Microscopy” in this Volume).

**Solidification Structures.** The most commonly observed solidification structure is dendritic (Fig. 24). A dendritic structure usually exhibits compositional variations, with the primary, secondary, and tertiary dendrite arms containing less alloying or impurity elements than interdendritic regions. Because of such

compositional changes (termed “*coring*”), the rate of etching at interdendritic regions differs from that at dendrite arms. If the alloying element or impurity content is high, interdendritic regions may develop a two-phase structure. Because dendrite arm spacing tends to decrease with increasing cooling rates, the properties of as-cast metals depend on the solidification rates.

Most metals shrink during solidification. Therefore, the liquid trapped between dendrite arms during solidification is frequently insufficient to fill the space between the arms when solidification is complete. This inability to fill the remaining space leads to shrinkage voids, which can be observed microscopically. Voids are generally easier to observe on as-polished specimens than on polished and etched ones. Figure 25(a) shows a typical example of shrinkage voids.

**Discontinuities.** Various materials discontinuities, such as inclusions and stringers (Fig. 25b and 25c) can also be observed microscopically in as-polished specimens. Such imperfections as those shown in Fig. 25 can serve as failure-initiation sites in metals and alloys; therefore, characterization of their size, shape, and distribution is necessary to establish material properties and

engineering reliability. Quality-assurance programs frequently require controlling imperfections to regulate their type, number, size, and shape in a particular manner. For example, a component having a stringer distribution such as that shown in Fig. 25(c) would have better ductility if specimens or components were tested with the major stresses parallel to the stringer than if specimens were oriented with the major stresses perpendicular to the stringer.

**Transformation structures** often consist of two phases. In such structures, the major phase is typically termed the matrix, or base structure, and the minor phase is termed the second phase. The size, shape, and distribution of second-phase particles are important in determining the properties of metals and alloys. Characterization of second-phase morphology can sometimes be accomplished using optical metallography. However, the second phase is sometimes so small that the resolution necessary to characterize the phase morphology exceeds the limits of the light microscope. In these cases, SEM may be used, or transmission electron microscopy may be needed. Age-hardenable or precipitation-hardened metals and alloys generally must be characterized using electron microscopy.



**Fig. 23** Same alloy and processing as in Fig. 22, but reduced 50% by cold rolling from 6 mm (0.239 in.) to 3 mm (0.120 in.). Grains are elongated in the rolling direction. Diagrams indicate same orientation of view as in Fig. 22. Etched using  $\text{NH}_4\text{OH}$  plus  $\text{H}_2\text{O}_2$ .  $75\times$ . Source: Ref 8

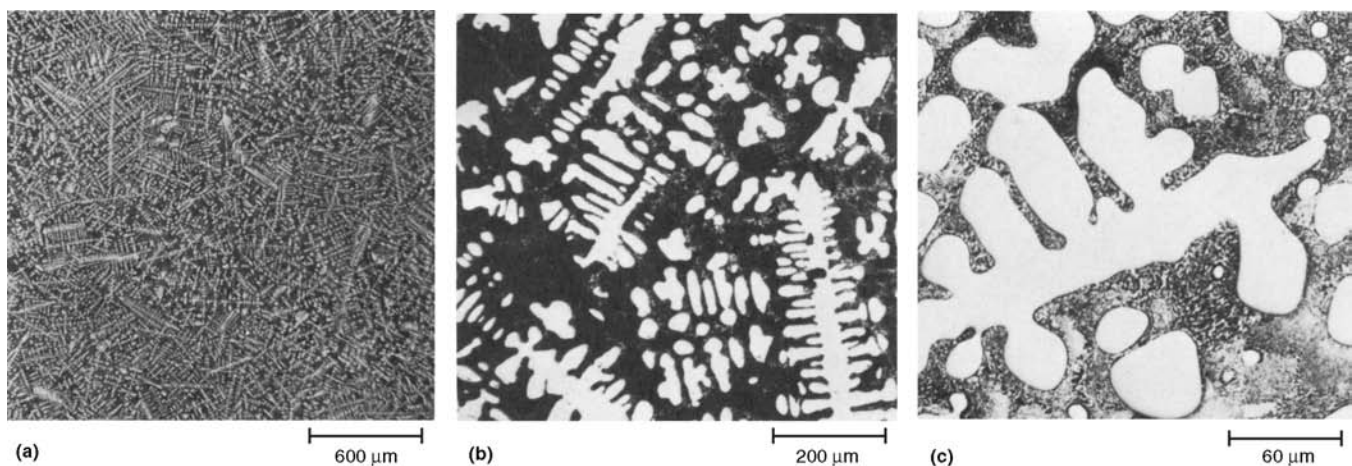


**Fig. 24** Dendritic solidification structure in a Ni-5Ce (at.%) alloy. Nickel dendrites (light in b and c) are surrounded by a matrix of nickel-cerium eutectic. (a)  $25\times$ . (b)  $75\times$ . (c)  $250\times$ . Source: Ref 8

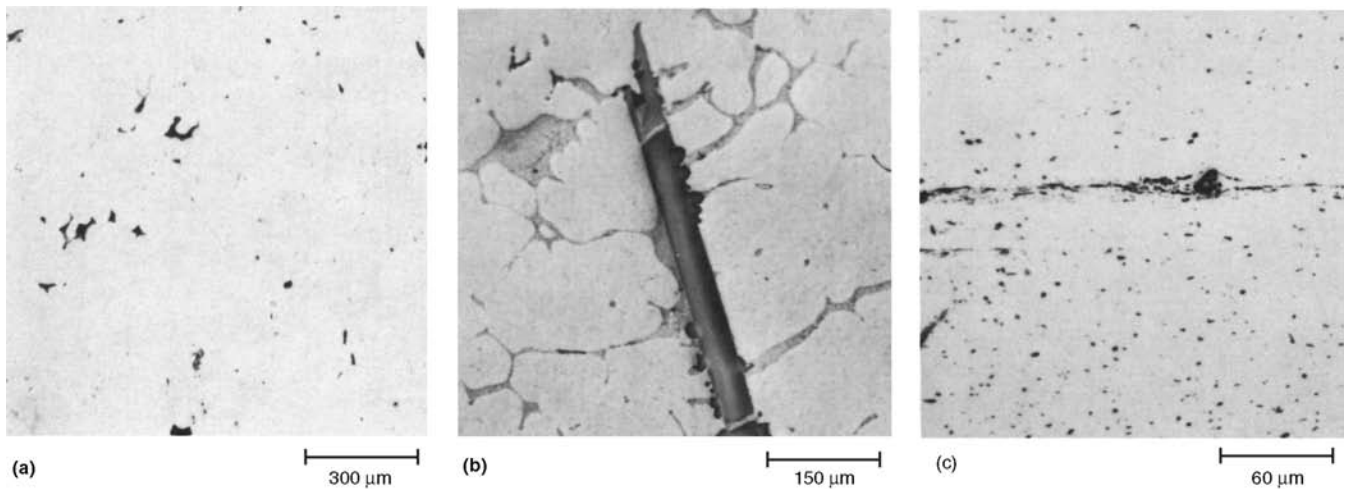


**Fig. 25** Typical imperfections observable using optical microscopy. (a) Shrinkage porosity in an aluminum alloy 5052 ingot. Note angularity. 50 $\times$ . (b) Coarse primary CrAl<sub>3</sub>-crystal in aluminum alloy 7075 ingot. 100 $\times$ . (c) Oxide stringer inclusion in a rolled aluminum alloy 1100 sheet. 250 $\times$ . All as-polished. Source: Ref 8

High-temperature phase transformations frequently nucleate at grain boundaries. The grain-boundary structures can be discrete or continuous. Continuous grain-boundary constituents (Fig. 26) provide easy fracture paths when the grain-boundary phase is less ductile than the matrix phase. For the material shown in Fig. 26, the expected failure would be fracture along the grain-boundary carbides. Heterogeneous precipitation at grain-boundary regions is typically based on the classic mechanism of precipitate nucleation and growth, where the initial nucleus starts at critical size to allow reduction in the interfacial surface energy between the precipitate and parent phases (see the article “Structures by Precipitation from Solid Solution” in this Volume). The transformation processes may also be continuous (e.g., see the article “Spinodal Transformation Structures” in this Volume).

**Deformation Structures.** The microscopic details of deformation structures typically cannot be fully established using light metallography. Deformation changes the number and arrangement of dislocations (crystal defects) in the metal on an atomic scale. This dislocation substructure is best characterized using TEM. Light-microscope metallography can be used to supplement TEM through characterization of the grain size and anisotropy in grain shape and distribution. Microstructural changes due to annealing can be studied using TEM or light microscopy. The most important structural changes that occur during annealing are recovery, recrystallization, and grain growth.

Recovery is the rearrangement and annihilation of imperfections (primarily vacancies and interstitials) within each grain of a cold-worked polycrystalline component. Because recovery deals mainly with point defects, any microstructural observations of it are difficult, and light microscopy cannot be used because of its limited resolution.

Recrystallization is the formation of new strain-free grains within the previously cold-worked (strained) grains. The initial stages of re-

crystallization occur on such a fine scale that TEM is necessary; however, light-microscope metallography can be readily used to study most of the recrystallization. The size of the recrystallized grains depends on the amount of cold working of the specimen before the recrystallization anneal. The greater the amount of cold work, the finer the recrystallized grain size (Fig. 27). Because grain boundaries are a crystalline defect, continued annealing will cause this array of grains to be unstable, and grain growth will take place. Grain growth in a recrystallized specimen decreases the grain-boundary surface area to specimen volume ratio because the average grain size increases as grain growth takes place. The rate of grain growth depends on temperature and time.

### Microfractography (Adapted from Ref 13)

Microscopic examination of the fracture surface is best accomplished by use of the scanning

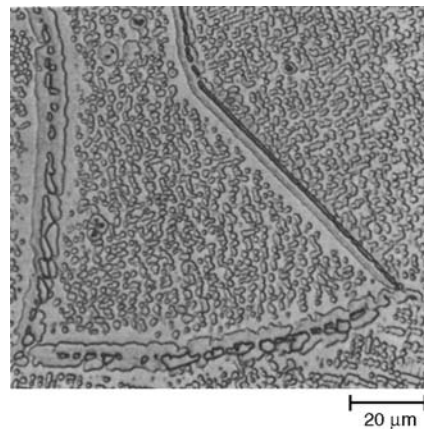


**Fig. 26** Continuous grain-boundary precipitate in U-700 nickel-base heat-resistant alloy. Etched using HCl, ethanol, and H<sub>2</sub>O<sub>2</sub>. 500 $\times$ . Source: Ref 8

electron microscope (SEM) and in some cases by examination of replicas with the transmission electron microscope (TEM). The SEM images in Fig. 28 show the distinctive microscopic features of the three basic types of overload fracture: transgranular brittle fracture (cleavage), transgranular ductile fracture (microvoid coalescence), and brittle fracture by intergranular separation. The SEM provides good depth of focus to observe topological features of the fracture surface. Modern SEM instruments also typically have x-ray spectroscopic attachments that allow elemental analysis of constituents on (or near) the specimen surface. This can be very helpful in failure analysis.

However, lack of access to a SEM or TEM should not be viewed as a crippling obstacle to performing failure analysis, because such work was done successfully prior to the development of these instruments. In many studies, such equipment is not needed, while in other cases, they are very important tools. In most cases, electron microscopy and light microscopy should be considered complementary tools. Microstructural examination can be performed with

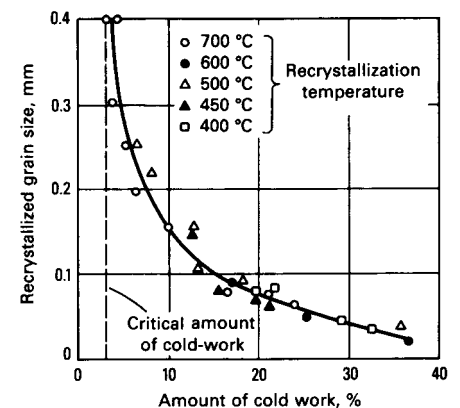


**Fig. 27** The effect of prior cold work on recrystallized grain size. Source: Ref 8